Available online at www.CivileJournal.org

Civil Engineering Journal

(E-ISSN: 2476-3055; ISSN: 2676-6957)

Vol. 12, No. 05, May, 2026

Predicting Temperatures in an Extreme Climatic Environment Using Hybrid Neural Networks: Evaluating Noise Robustness

Ali W. Alattabi [1*], Salah L. Zubaidi [1, 2*], Hussein Al-Bugharbee [3], Hussein Mohammed Ridha [4, 5], Mawada Abdellatif [6], Hassimi Abu Hasan [7, 8, 9]

[1] *Department of Civil Engineering, Wasit University, Wasit 52001, Iraq.*

[2] *College of Engineering, University of Warith Al-Anbiyaa, Karbala 56001, Iraq.*

[3] *Department of Mechanical Engineering, Wasit University, Wasit 52001, Iraq.*

[4] *Advanced Lightning, Power and Energy Research (ALPER), Department of Electrical and Electronics Engineering, Faculty of Engineering, Universiti Putra Malaysia, Serdang 43400, Malaysia.*

[5] *Department of Computer Engineering, University of Al-Mustansiriyah, Baghdad 14022, Iraq.*

[6] *Department of Civil Engineering and Built Environment, Faculty of Engineering Technology, Liverpool John Moores University, Byrom Street, Liverpool L3 3AF, United Kingdom.*

[7] *Department of Chemical and Process Engineering, Faculty of Engineering and Built Environment, Universiti Kebangsaan Malaysia, UKM, Bangi, Selangor 43600, Malaysia.*

[8] *Research Center for Sustainable Process Technology (CESPRO), Faculty of Engineering and Built Environment, Universiti Kebangsaan Malaysia, UKM, Bangi, Selangor 43600, Malaysia.*

[9] *Water and Wastewater Treatment Technology Research Group, Universiti Kebangsaan Malaysia, UKM, Bangi, Selangor 43600, Malaysia.*

Received 18 February 2026; Revised 19 April 2026; Accepted 23 April 2026; Published 01 May 2026

Abstract

Predicting maximum temperatures is crucial across many fields and industries, including medicine, agriculture, energy, and climate research. Researchers have not treated the prediction of maximum temperatures under severe artificial data disturbance in much detail. So, it has not yet been understood. This research aims to integrate an artificial neural network (ANN) with the Guaranteed Convergence Arithmetic Operation Algorithm (GCAOA) to forecast monthly maximum temperatures while ensuring robustness to noise. Univariate data from Al-Hai City over 12 years were employed to build and assess the model. The performance of GCAOA was examined and compared with that of the two hybrid ANNs, the random forest, and the XGBoost models. Across various input scenarios, the results reveal that these three hybrid models achieved very good forecast performance compared with random forests and XGBoost. The GCAOA-ANN (swarm size of 20 and lag2) achieves the best forecast performance among the hybrid algorithms across different statistical fitness measures with a coefficient of determination, Nash-Sutcliffe coefficient, and root mean squared error of 0.972, 0.969, and 1.7354°C, respectively. The performance of the hybrid ANN models was further investigated under noise, and the results showed the superiority of the GCAOA-ANN model.

Keywords: Temperature Forecasting Model; ANN; Metaheuristic Algorithm; SDGs; Noise Robustness; Signal-To-Noise Ratio (SNR).

1. Introduction

Weather prediction is crucial across sectors, including energy management, agriculture, disaster response, and transportation [1]. In particular, temperature plays a vital role in revealing how the planet and its atmosphere respond to

* Corresponding author: anakemish@uowasit.edu.iq; salahlafta@uowasit.edu.iq

https://doi.org/10.28991/CEJ-2026-012-05-017

climate change, more so than other meteorological variables. In the Middle East, Iraq faces significant aridity challenges, manifested in rising temperatures that threaten the environment and crop productivity. Temperature fluctuations are significant, with summer means exceeding 43 °C, whereas nighttime winter temperatures can drop to about 2 °C. Southern Iraq has recently seen heat waves reaching 50 °C, with record-breaking temperatures in Basra approaching 54 °C [2]. Moreover, according to a 2018 report by the Expert Working Group on Climate-Related Security Risks, climate change has led to prolonged heat waves and rising temperatures, which have become a substantial problem in southern Iraq [3].

Accurate temperature estimates support several Sustainable Development Goals (SDGs) and help to 1) evaluate potential climatic changes' effects and ensure risk mitigation, such as heat waves and droughts (SDG13). 2) reducing the heat island effect in cities and improving quality of life (SDG11). 3) assessing water demand and managing water resources, especially in arid regions (SDG6). 4) agricultural planning and effective irrigation management (SDG2) [4, 5].

Several factors are known to affect air temperature variations [6]. Hence, the rate of temperature change is neither static, predictable, nor linear [7]. Conventional numerical weather forecast techniques relied on tackling complicated physical equations that describe atmospheric dynamics. Though these techniques have advanced substantially, they still require substantial computational resources and may not detect nonlinear interactions and small-scale atmospheric processes [1]. However, Machine learning (ML) is outperforming traditional methods, providing new insights for meteorological science [8]. A large and growing body of literature has investigated ML models in predicting temperature data, for example:

Bhih et al. [1] examine three ML models for forecasting temperatures across five regions in Asia and Europe. These ML models are eXtreme Gradient Boosting (XGBoost), Categorical Boosting (CatBoost), and Light Gradient Boosting Machine (LightGBM). The performance of these ML models was assessed against deep learning models, including Long Short-Term Memory (LSTM) networks and hybrid LSTM with convolutional neural networks (CNN-LSTM). The results reveal CatBoost's superiority in achieving lower error. Gomes, et al. [9] proposed a feed-forward network (FF-ANN) model to estimate air temperatures. The air temperature dataset, with a 5-minute measurement interval, was collected over 2 years (2018 to 2020) in Brazil. The performance of the FF-ANN model compared with the LSTM model, and the findings indicate that FF-ANN is better based on the error scale. The study recommended applying the FF-ANN in different areas around the world.

Topcu, et al. [10] use six ML models to predict maximum temperatures in South Korea and Kuwait. These models are ANN, support vector regression (SVR), K-nearest neighbors (KNN), decision tree (DT), ridge regression, and random forest (RF). The results show that ANN and SVR achieve better performance than other models, with lower errors and less bias across both Kuwaiti and South Korean extremes. The comparative investigation shows that NN and SVR attain robust accuracy in forecasting, particularly for detecting nonlinear variations in temperature. Sevgin [11] assessed ANN, RF, SVR, KNN, and linear models for forecasting temperatures. The time series data was employed from 1950 to 2023 in Istanbul, Turkey. The outcomes show that the ANN technique achieved 96% accuracy. On the other hand, the RF technique attained the highest performance. The study recommended applying ANN and RF techniques for different regional climate studies.

Artificial neural networks (ANNs) are one of the ML models that play a crucial role in forecasting air temperature data [9]. The neural network revealed its ability to capture complicated patterns and relationships in temperature time series [10]. However, recent studies highlight the need to optimize hyperparameters of ML techniques to improve forecasting performance [11-13]. Accordingly, ANN models are recommended to be integrated with metaheuristic algorithms (MHAs), which have not been investigated in detail for air temperature forecasting.

Comparing hybrid approaches with standalone ML techniques, MHAs can solve many hard, nonlinear metrological problems [14-16]. These combined approaches are desirable for addressing complex real-world situations [17]. This is why these techniques have revealed improvement in detecting new locations, potentially leading to more solutions [18]. The capacity to exploit is also increased to avoid local minima. Finally, these approaches excel in complicated, nonlinear problems [19]. Nevertheless, optimization remains essential, particularly for predicting meteorological parameters, given their non-stationary, stochastic nature and data noise [7, 20]. Also, as hybrid models evolve across sectors, hybrid-based MHA (i.e., containing more than one strategy) outperforms single-strategy-based MHA [21-23]. Recently, the arithmetic optimization algorithm (AOA), which is a mathematical optimization, was hybridized with multiple techniques to improve the performance of its strategy and applied successfully in different areas, including Guaranteed Convergence Arithmetic Operation Algorithm (GCAOA) [24], Improved Arithmetic Optimization Algorithm (IAOA) [25], and Hybridized Arithmetic Operation Algorithm (HAOA) [26].

The atmosphere's inherent volatility and unpredictability make accurate weather prediction a formidable task. Consequently, reliable information for future planning can only be obtained from accurate, timely maximum temperature forecasts [27, 28]. Accordingly, maximum temperature forecasts have recently attracted significant attention from

scientists due to their many positive effects on the environment and the economy. However, reviewing air temperature modeling methods over the past few decades [29-32] revealed that these studies have not addressed the assessment of prediction performance under severe artificial data disturbance in much detail. Thus, most of the criticism remains, and it has not been fully understood.

Considering the constraints identified in the literature review, this research aims to develop and validate a robust predictive framework for maximum temperature forecasting in Al-Hai City, Iraq, utilizing 12 years of monthly time-series data. The methodology begins by establishing six distinct input combination scenarios derived from historical observations to identify the most sensitive variables influencing the target output. To enhance forecasting precision, a novel hybrid algorithm, GCAOA-ANN, is evolved and subsequently benchmarked against two other hybrid models, IAOA-ANN and HAOA-ANN. The RF and XGBoost models are then applied to assess the performance of hybrid ANN models. To address the inherent challenges of forecasting range and uncertainty, the study employs an iterative approach, conducting three repetitions for each swarm size across all algorithms. Finally, the robustness and stability of the proposed models are rigorously evaluated by introducing artificial noise at signal-to-noise ratios (SNR) of 20, 25, and 30 dB, ensuring the models maintain high predictive accuracy and generalizability even under suboptimal data conditions.

2. Methodology

This study proposes a novel methodology dedicated to understanding the forecast of monthly maximum temperature based on six predictor combination scenarios (see Figure 1). The proposed study methodology began with data collection in Al-Hai City, Iraq. Then, developing six predictor combination scenarios. The next step was partitioning the data into three categories: training, validation, and testing. Following that, the model configuration stage involved combining the ANN with three MHAs to determine the best hyperparameters for the ANN. The next step was to carry out the performance assessment of the forecasting techniques review. This is the point where all the models are run. In the last step, the models are evaluated using several statistical and graphical tests to choose the most effective forecast model. The following sections (i.e., 2.1-2.5) describe the methodology.

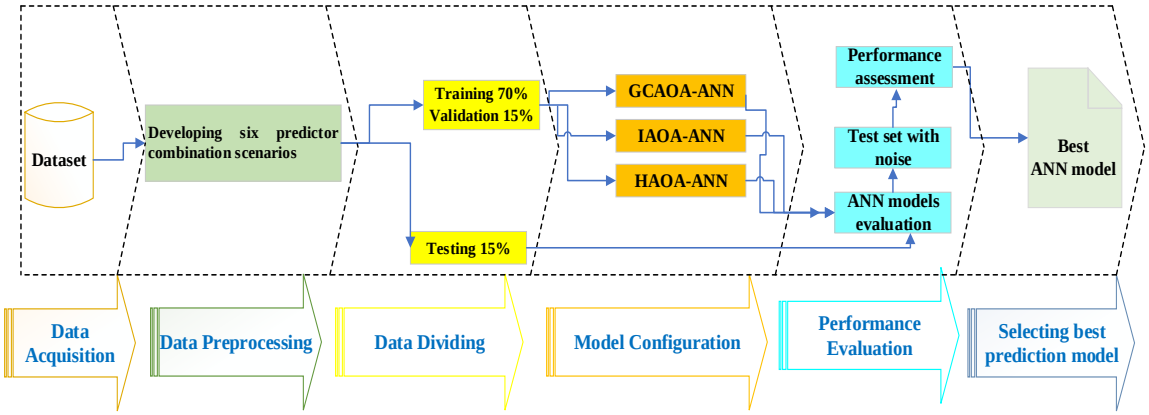

Figure 1. Methodology framework of the proposed study

2.1. Study Area

The total land area of Iraq is around 438,314 km². Except for the hilly regions in the north and northeast, most of Iraq experiences a continental and subtropical climate [33]. A Mediterranean climate characterizes the mountainous area. December through February, or November through April, is the typical rainiest period in the mountainous area. Daytime highs of around 16 °C drop to 2 °C at night, and frost is possible during the chilly to cold winters. Temperatures dip to 25 degrees Celsius at night during the dry, hot summer months but reach 45 degrees Celsius in the shade in July and August [34]. Al-Kut City is on the banks of the Tigris River in southeastern Iraq and serves as the provincial capital of Wasit. Located between 32° 21" and 32° 34" north and 45° 54" and 45° 45" east longitude, it is about 20 meters above sea level on average [35]. Extremely cold winters and dry, hot summers characterize Wasit Province's continental and semiarid climate. In July and August, the average daily temperature can reach 51 °C. Between 150 and 300 millimeters of precipitation falls each year [36]. With an area of about 40 square kilometers, Wasit Province is well known for its wheat production [36].

Recent studies using satellite data to assess future climate change have shown that temperatures are likely to increase across Iraq [37-40] under different emission scenarios, especially in the middle and southern parts [3, 41, 42]. The area of study was chosen for its importance, as it is the largest district in Iraq and the main city for strategic crops. Also, the city reflects the pattern of arid to semi-arid environments in middle and southern Iraq, which experience particularly high summer temperatures. In addition to the city's importance, the availability of continuous climate data in Iraq is one

of the most significant challenges for research. Monthly maximum temperature data for Al-Hai City, part of Wasit Province, from 2005 to 2016 are utilized in this study. Figure 2 shows a box plot of the maximum temperature with a normal distribution curve. Mean, median, first and third quartiles, as well as upper and lower whiskers, are all displayed in the figure. There are also no outliers in the series period.

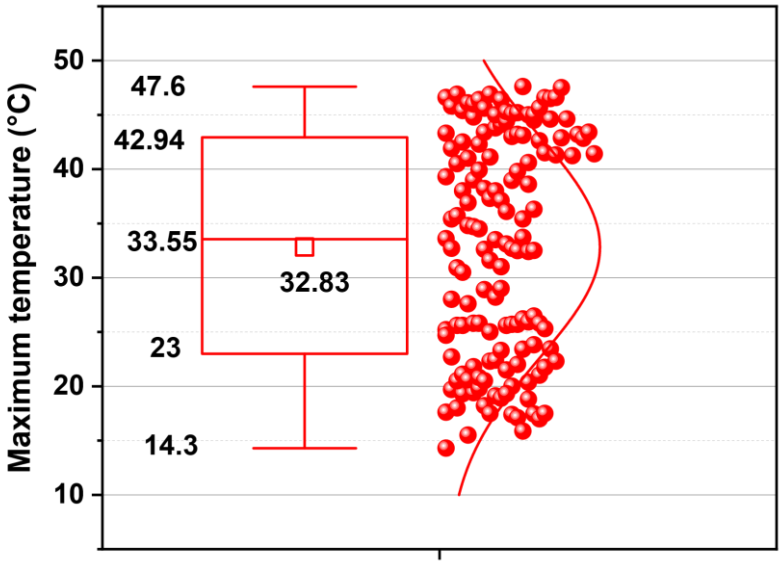

Figure 2. A box plot of the maximum temperature with a normal distribution curve

2.2. Arithmetic Optimization Algorithm (AOA)

The arithmetic optimization algorithm (AOA) can be categorized as a population-based optimization technique [25]. The main procedure of all stochastic algorithms is exploration and exploitation. The search space must be explored extensively in order not to be trapped in local optima. In the exploitative stage, even slight changes in the values of the variable could lead to divergence. Therefore, finding the best algorithm requires striking a balance between the two phases of development. The math operators of arithmetic algorithm are: multiplication ‘‘×’’, division ‘‘÷’’, subtraction ‘‘-’’, and addition ‘‘+’’.

The aforementioned math operators of arithmetic algorithm are widely used in different computational sciences [43]. In a study of proton exchange membrane fuel cell (PEMFC), AOA was applied successfully to obtain the optimal model identification [44]. Thus, the best solutions could be discovered by modifying the four math operators while maintaining a balance between the exploration and exploitation stages [45].

Initially, a collection of possible solutions (X) is produced at random by implementing the initialization stage. The ideal solution, which is the best after all iterations, is saved.

$$X = \begin{bmatrix} X1,1 & \ldots. & \ldots. & X2,j & X2,1 & X2,1 \\ X2,1 & \ldots. & \ldots. & X2,j & \ldots\ldots & X2,n \\ \ldots\ldots & \ldots. & \ldots. & \ldots\ldots & \ldots\ldots & \ldots\ldots. \\ \ldots\ldots & \ldots. & \ldots. & \ldots\ldots & \ldots\ldots & \ldots\ldots. \\ \ldots\ldots & \ldots. & \ldots. & \ldots\ldots & \ldots\ldots & \ldots\ldots. \\ \ldots\ldots & \ldots. & \ldots. & \ldots\ldots & \ldots\ldots & \ldots\ldots. \\ XN-1,1 & \ldots. & \ldots. & XN-1j & \ldots & XN-1,n \\ XN-1 & \ldots. & \ldots. & Xnj & XN,n-1 & XN,n \end{bmatrix} \quad (1)$$

In this case, x is the solution vector, n is the number of dimensions, and number of search agents is denoted by N. The AOA uses a function called Math Optimiser Accelerated (MOA), which can be computed as follows, to define the exploration and exploitation stages.

$$\mathrm{MOA}(C_{iter}) = Min + C_{iter} \times \left(\frac{Max-Min}{M_{iter}}\right) \quad (2)$$

where, MOA(C_{iter}) is the value of the function at the *t* th iteration, and C_{iter} is the current iteration, both of which can take values between 1 and the maximum iteration number, M_{itre}. Those are the lowest and highest points of the accelerated function, respectively.

It is during this experimental phase that the AOA division (D) and multiplication (M) operators are utilized, because their values in design space are very dispersed. Conversely, the D and M mechanisms have a high dispersion capacity, which makes it more difficult to get close to the target.

The exploration stage is dependent on the MOA function, if the value of r_1 , which is picked at random, higher than the MOA, the D and M operators are utilized; otherwise, A and S operators are used. The equation of the exploration stage is described as follows:

$$X_{i,j}(C_{iter}+1)=\begin{cases} best(X_j)\div(MOP+\epsilon)\times\left(\left(UB_j-LB_j\right)\times\mu+LB_j\right) & r2>0.5 \\ best(X_j)\times MOP\times\left(\left(UB_j-LB_j\right)\times\mu+LB_j\right) & otherwise \end{cases} \quad (3)$$

For operators D and M, r_2 is a number chosen at random. The lower and upper limit values of the j th position are denoted by UB_j and LB_j, respectively. μ is a control value set to 0.5 to maintain the search method, and ϵ is a small numerical value.

The exploitation stage is operated by using addition (A) and subtraction (S) operators. Despite their high density work, the A and S are easily approachable because of their low dispersion. The A and S are modelled as follows:

$$X_{i,j}(C_{iter}+1)=\begin{cases} best(X_j)-MOP\times\left(\left(UB_j-LB_j\right)\times\mu+LB_j\right) & r3>0.5 \\ best(X_j)+MOP\times\left(\left(UB_j-LB_j\right)\times\mu+LB_j\right) & otherwise \end{cases} \quad (4)$$

In this case, the A and S operators are distinguished by a randomly chosen number r_3.

2.2.1. Improved Arithmetic Optimization Algorithm (IAOA)

During the problem's optimization, the AOA randomly uses four arithmetic mathematical operations, which leads to the loss of numerous optimal solutions and makes it harder to escape from local minima. It has been noted that the population is frequently updated at random, utilizing lower and upper bound variables within the framework of the four processes.

Because of the mathematical models used in these four operations, the introduction of the population is compelled to be random and strategy- and strength-free. Finding an equilibrium between the two phases of exploration and exploitation is important, but so is increasing the population's diversity for the sake of discovering untapped regions of promise and going above and beyond the previous solution to ensure that the population is of high enough quality. Given the aforementioned limitations, the original AOA has been enhanced by applying the following tactics [25]:

Finding new regions in the search space requires a strong strategy, which can be obtained with the generalized opposition learning technique (GOL) [46]. Stochastic techniques have been widely integrated with GOL, a relatively new field of study, to improve its performance [47]. The GOL's mathematical model can be expressed as follows:

$$X_{i,j}^{GOL}=rand\times(A_j+B_j)-xnew_{i,j}\,;where\colon X_{i,j}^{GOL}\,\epsilon\left[A_j,B_j\right];j=1,2,\ldots.,D \quad (5)$$

The minimum and maximum numbers of the current iteration are denoted by Aj and Bj, respectively. The result is that GOL promotes up convergence and increases the algorithm's leap from locality [48].

The control parameter for step size is crucial for maintaining exploration-exploitation balance. Convergence is accelerated with a big search step size and improved with a small step size [49]. The following represents the enhanced nonlinear step size:

$$L=\frac{2}{1+\exp\left(\frac{10*N-i}{M_{iter}-C_{iter}}\right)} \quad (6)$$

where, N represent the size of population. The L value in the abovementioned equation starts out high and declines as the iteration goes on.

During the entire process of optimisation, variables representing the bottom and upper limits from the previous modelling of the four arithmetic processes are used to produce new solutions. Numerous potential solutions are lost during this operation, and population updating is always done at random. In the new model of the four arithmetic operators, two groups of vectors are chosen at random from the existing population after a sequence of random integers (dm) is dispersed according to the length of the population [48]. The current solution (x_i) for the S and D operators is retained by merging it. On the other hand, the best solution (best) yields the A and M operators. This allows for the updating of the diversity of solutions through the use of S and D operators (exploration stage), and the execution of the highest quality solution through the use of A and M operators (exploitation stage). The four arithmetic operators are modelled as follows:

$$X_i(C_{iter}+1)=\begin{cases} X_i-MOP\times\left(\left(X_{dm1}-X_{dm3}\right)\times L\right) & r3>0.5 \\ best+MOP\times\left(\left(X_{dm1}-X_{dm2}\right)\times L\right) & otherwise \end{cases} \quad (7)$$

Among the many robust techniques available to the differential evolution (DE) method, mutation stands out for its ability to both globally check search directions and improve solution quality with fewer iterations [50]. The exploration or exploitation tendencies formula can be utilized to create a variety of DE schemes [51]. The following two techniques were used: DE/current/1 and DE/best/2:

$$X_i(C_{iter}+1) = xnew_i - rand \times (X_{dm1} - X_{dm2}) \tag{8}$$

$$X_i(C_{iter}+1) = \text{best} - L \times \left((X_{dm1} - X_{dm3}) + (X_{dm1} - X_{dm2})\right) \tag{9}$$

The most effective mutation strategy is selected based on which fitness function is the lowest. Stated differently, the proposed IAOA functions in two ways, leveraging mutation processes and simultaneously obtaining the advantages of local and global search [52]. Eventually, this operation will be carried out again until the stopping requirement is satisfied.

2.2.2. Hybridized Arithmetic Optimization Algorithm (HAOA)

One of four arithmetic mathematical operations is carried out in the basic AOA during each iteration of the random mechanism-based program. Because of this, finding an acceptable balance between the exploration and exploitation phases is impossible. Furthermore, the addition and multiplication operators are unavailable during the exploration and exploitation phases [26]. Taking into consideration the numerous constraints present in the original AOA to enhance the quality of optimal solutions, new methods for finding new regions have been presented.

The four arithmetic mathematical operations have been utilized to divide the population into two groups. The exploration part is shown below:

$$X_{i,j}(C_{iter}+1) = \begin{cases} best(X_j) \div Mu \times \left((UB_j - LB_j) \times RL_{i,j} + LB_j\right) & r2 > 0.5 \\ best(X_j) \times rand \times \left((Bst_j - X_{i,j}) - Mu \times rand \times (Wrst_j - X_{i,j})\right) & otherwise \end{cases} \tag{10}$$

where Mu is presented by:

$$Mu = 2e^{-\left(\frac{4C_{iter}}{M_{iter}}\right)^2} \tag{11}$$

Therefore, Mu significantly affects the early phases of optimization by increasing diversity and the later stages of optimization by assuring intensification. In the Levy flight method, $RL_{i,j}$, the step sizes are chosen at random using a probability function and are provided by Humphries et al. [53].

$$RL_{i,j} \approx |L_j|^{1-\alpha} \tag{12}$$

In cases where L_j is the flight duration, the power-law exponent falls within the range of 1 to 2 [53]. Here is the value of the Levy distribution's probability density expressed in integral form Mantegna [54]:

$$f_L(x, \mu, \sigma) = \frac{1}{\pi} \int_0^{\infty} \exp(-\gamma q^{\alpha}) \cos(qx)\, dq \tag{13}$$

The distribution index α controls the scale features of the process, and the scale unit is chosen using γ. When α=1 denotes a Cauchy distribution and when α=2 denotes a Gaussian distribution, the integral is employed [54].

To prevent getting stuck in locality and make sure the decision-making process uses the most optimal solutions, the A and S operators in the enhanced exploitation stage need to get the very small step size of the Mu mechanism and the stochastic step size of the Brownian motion (RB), respectively. Next, to increase the variety of the best global solution to date and local optimal avoidance, we choose the best current optimum solution (Bst_j) instead of the best optimal global solution (best(X_j)), as demonstrated below:

$$X_{i,j}(C_{iter}+1) = \begin{cases} best(X_j) \div Mu \times \left((UB_j - LB_j) \times RB_{i,j} + LB_j\right) & r2 > 0.5 \\ best(X_j) \times rand \times \left((Bst_j - X_{i,j}) - Mu \times rand \times (Wrst_j - X_{i,j})\right) & otherwise \end{cases} \tag{14}$$

Following the exploration and exploitation stages, the first half of generations utilized the chaotic distribution to effectively find new locations in the search space while avoiding local solutions [55, 56]. Additionally, this randomized search technique aims to accelerate convergence in a limited number of generations, as follows [18]:

$$X_{m+1} = 4\,.X_m(1 - X_m) \tag{15}$$

where;

$$X_i(C_{iter}+1) = best\left(X_j\right) + rand\,.\,(2\,.X_m - 1) \quad (16)$$

Eventually, this process will be iterated until the halting condition is met.

2.2.3. Guaranteed Convergence Arithmetic Optimization Algorithm (GCAOA)

Because of the original mathematical models that are obtained during both the exploration and exploitation stages, the basic AOA has many limitations. Particularly when dealing with complicated, multi-dimensional, or high-dimensional optimization procedures, this causes a decrease in its performance. Consequently, the suggested improvements attempt to ensure convergence for the best solutions at every execution.

When optimization begins, the worst solution is discarded and replaced with the best one. Until the end of the generations, this process will be carried out. The following are the enhancements to the suggested GCAOA [24]:

According to the exploratory stage, the population has been divided into two categories, utilizing four arithmetic operators:

$$X_{i,j}(C_{iter}+1) = \begin{cases} best(X_j)\bar{\mathrm{A}}\,.\,(Mu+\epsilon) \times \left(\left(UB_j - LB_j\right) \times RL_{i,j} + e_j\right) & r2 > 0.5 \\ best(X_j) \times rand \times \left(\left(Bst_j - X_{i,j}\right) - Mu \times rand \times (Wrst_j - X_{i,j})\right) & otherwise \end{cases} \quad (17)$$

where, *Mu* can be found through Equation 11, $RL_{i,j}$ can be found through Equation 12

In particular, when working with the Gaussian distribution and Levy flight approaches, the S operator is crucial for traversing from local to global levels. The A operator allows decision-making in obtaining the most successful outcome given neighborhood data by utilizing the short step size of the Mu mechanism.

$$X_{i,j}(C_{iter}+1) = \begin{cases} best(X_j) - Mu \times \left(\left(UB_j - LB_j\right) \times RL_{i,j} + e_j\right) & r2 > 0.5 \\ best(X_j) + F_1 \times \left(\left(Bst_j - X_{i,j}\right) - F_2 \times (Wrst_j - X_{i,j})\right) & otherwise \end{cases} \quad (18)$$

Some of the recently produced solutions went beyond the optimization problem's upper and lower bounds since the optimization procedure used a lot of random techniques. The majority of optimization algorithms yield straightforward lower and upper bounds, which may result in slowing the rate at which optimal solutions converge. Using the following mathematical model, a new mechanism has been proposed to tackle this problem by transforming the particle from predefined lower and upper bounds to nearest-optimum areas:

$$X_{i,j} = best\left(X_j\right) + \epsilon \times \left(rand \times \left(UB_j - LB_j\right)\right) \times rand \times LB_j \quad (19)$$

The formulas discussed earlier greatly increase the diversity of the best optimal solutions found so far. In other words, not only are particles relocated to more ideal locations, but data from the area around the best particle is also used to improve solution quality.

The Generalized Opposition Learning (GOL) strategy gained up to one third of generations to effectively identify the farthest area of the search space after the exploration and exploitation stages are finished [46]. By adding random steps of the Levy flight (RL) strategy, the GOL is enhanced. This strategy can significantly improve the diversity of the solutions and has a unique ability to transition from a locality to previously unexplored areas [46]. The improved (IGOL) is modeled as follows:

$$X_{i,j}^{IGOL} = xnew_i + RL_i \times \left(rand \times \left(A_j - B_j\right) - xnew_i\right); \quad (20)$$

where;

$$X_{i,j}^{IGOL} \epsilon \left[A_j - B_j\right]; j = 1,2,\ldots.,D \quad (21)$$

The current iteration's minimum and maximum values are A_j and B_j, respectively. *RL* is levy flight strategy. As a result, IGOL prevents the algorithm from becoming too focused on a single area or converging too soon [48].

2.3. Artificial Neural Network

Predictions of air temperature using ANN models have generally been accurate and promising. A multi-layer perceptron is a feed-forward (MLP-FF) ANN model that has seen extensive use in this field. The ANN is also expected to impact air temperature forecasting going forward significantly [30]. ANNs have a wide range of applications due to their ability to capture highly nonlinear correlations and map complex input-output rules in data [57]. For the purpose of training the ANN, the Levenberg-Marquardt (LM) algorithm was chosen due to its shown ability to minimize

prediction error and accurately replicate any predictor/response map [58, 59]. Similarly, among the documented activation function combinations, tansigmoidal for the hidden layer and pure linear for the output layer is the most commonly utilized [60].

Many studies have successfully employed two-hidden-layer ANNs in a variety of contexts, demonstrating that these approaches reliably anticipate the nonlinear association between predictors and targets [61]. A four-layer artificial neural network was constructed; two hidden layers were added for data processing, and finally, an output layer was made for the final prediction (maximum temperature). The input layer was designated for independent variables (six Lags scenarios). Consistent with previous research [62], the dataset was partitioned into a training set (70%), a validation set (15%), and a test set (15%) of the remaining data.

The ANN learning process undergoes many iterations (about 1000) per epoch until the forecast-measurement error is as small as possible [62]. The optimal result is not invariably achieved using the trial-and-error approach. The optimal number of neurons in the initial (N1) and second (N2) hidden layers, together with the ideal learning rate (LR), were determined using several metaheuristic methods combined with artificial neural networks to achieve the most accurate independent/dependent mapping and mitigate over- and underestimation. This study will utilize the Improved Arithmetic Optimization Algorithm (IAOA), Hybridized Arithmetic Operation Algorithm (HAOA), and Guaranteed Convergence Arithmetic Operation Algorithm (GCAOA) in conjunction with ANN to reduce uncertainty and enhance the forecasting range.

2.4. Adding Artificial Noise and Testing Model Robustness

To assess the robustness of the proposed predictive models and avoid limiting the evaluation to ideal data conditions, an additional test was conducted by adding artificial noise to the test data. Three noise sets with different signal-to-noise ratios (SNR) were selected (20, 25, and 30 dB), spanning from relatively low noise to a severe disturbance scenario, to simulate potential uncertainties in the input data. Due to the random nature of noise generation, each SNR level was implemented 10 times independently, and the statistical performance indicators were calculated as the arithmetic mean of these realizations to minimize the effect of random fluctuations and enhance the reliability of the results. This procedure tests the robustness and predictive stability of the models and evaluates their ability to maintain accuracy and generalizability when dealing with noisy data.

2.5. Model Validation

This study employed many performance metrics to evaluate the model's efficacy. In the absence of a broadly appropriate efficiency metric, it is crucial to select the right parameters for a specific application. Furthermore, it is customary to employ many performance metrics owing to the advantages and disadvantages inherent in each criterion [63]. Additionally, performing various statistical tests helps confirm the superiority of the given methodology [64]. This research employs various performance criteria, including root mean squared error (RMSE), Nash-Sutcliffe coefficient (NSC), maximum error, mean absolute error (MAE), mean absolute relative error (MARE), normalized mean square error (NMSE), and coefficient of determination (R^2). The model's accuracy and fit quality improve as the R^2 value approaches 1. The NSE serves as an effective metric for model performance when it approaches 1, a principle that also applies to NMSE and R^2. Conversely, MAE and RMSE should ideally be zero to indicate optimal model performance [65-67]. Additionally, other graphical assessments were employed to evaluate the methods, including the Taylor diagram correlation coefficient (R), error scatter plot, and time series comparison.

3. Results

This section can be divided into two parts: model configuration and performance assessment of forecasting techniques. The primary focus of the first section will be the role of the three MHAs in determining the optimal hyperparameters for ANNs, selecting the swarm that minimizes the fitness function (RMSE) for each case. In the second section, various graphical tests and statistical criteria are used to identify the hybrid technique with the lowest error and higher correlation for forecasting the maximum monthly temperature. Moreover, the performance of hybrid models was confirmed by comparing them with those of RF and XGBoost techniques.

3.1. Models' Configuration

The 12-year monthly maximum temperature time series shows no outliers in the box-and-whisker plot (Figure 2). According to Wang et al. [31], the study recommended maximizing the model input range to exploit utilization in ML applications. In this research, Table 1 presents the model input combinations and targets for each of the six scenarios. It can be seen from the table that the first model is simple, while the others involve multiple inputs. The model input is represented by one or more of the lagged versions of the original time series. The target, or output, is represented by the current temperature. In general, for each scenario, the entire model aims to relate the current value of maximum temperature to a different number of past values.

Table 1. The maximum temperature input design

Models' name	Input combination	Target
M1	T_{lag1}	T_t
M2	T_{lag1}, T_{lag2}	T_t
M3	T_{lag1}, T_{lag2}, T_{lag3}	T_t
M4	T_{lag1}, T_{lag2}, T_{lag3}, T_{lag4}	T_t
M5	T_{lag1}, T_{lag2}, T_{lag3}, T_{lag4}, T_{lag5}	T_t
M6	T_{lag1}, T_{lag2}, T_{lag3}, T_{lag4}, T_{lag5}, T_{lag6}	T_t

Designing the hybrid prediction model is crucial for accurately estimating the maximum temperature time series. As mentioned earlier in this research, the ANN technique is combined with various MHAs to determine the optimal set of ANN hyperparameters, including the learning rate and the number of neurons in the two hidden layers. These MHAs are GCAOA, HAOA, and IAOA. It is vital to develop the forecasting technique methodically to accurately estimate temperature after splitting the data into training, validation, and test sets. The combined models are trained to relate the outputs to one or more model inputs. These model inputs are formed by lagging the original temperature time series by up to 6 lags.

For a fair comparison, all algorithms are set with a maximum number of 200 iterations. The swarm number increases to 10, 20, 30, 40, and 50 at each series lag. The hybrid algorithms are run three times at each lag and swarm size to reduce the effect of uncertainty and increase the forecasting range. So, the total number of runs for each hybrid model will be 90 (i.e., 6 lags × 5 swarm groups × 3 run times per swarm). For all these configurations, the model hyperparameters are determined where the loss function (RMSE) is minimum. For example, Figure 3 shows the training time history of the GCAOA-ANN model using the lag2 scenario (M2) of the time series with different swarm numbers. The x-axis represents the number of iterations (i.e., 200), while the y-axis represents the loss function (RMSE). From this figure, it is clear that the minimum RMSE is obtained with a swarm size of 30.

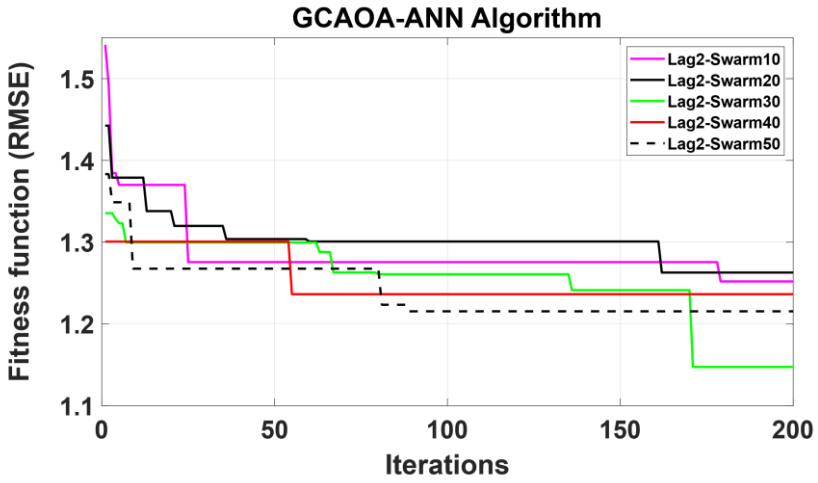

Figure 3. The optimal swarm for maximum temperature modelling using the GCAOA-ANN algorithm under the M2 scenario

Other MHAs (i.e., HAOA-ANN and IAOA-ANN) are applied to validate the GCAOA-ANN's outcomes. Figure 4 shows the configuration process for each of the three MHAs at the optimal number of lags and swarms. Generally, for the same number of iterations, it is clear that the Lag1 version of the time series is poorly predicted by all three hybrid algorithms, with the fitness function being the highest among the Lag versions. This might reflect lag1's lack of information. On the other hand, the lag2 version of the time series is accurately predicted in all three hybrid algorithms. Closer inspection of GCAOA-ANN reveals that the convergence rates between lags 4, 5, and 6, and between lags 2 and 3, were very comparable. However, lag 2 with 30 swarms exhibited the lowest RMSE. The HAOA-ANN shows that the convergence rates between lags 4, 5, and 6 were very comparable, whereas those between lags 2 and 3 were less comparable. However, lag 2 with 40 swarms exhibited the lowest RMSE. The IAOA-ANN reports that convergence rates for lags 4, 5, and 6 were higher than those for lag 3, while lag 2, with 20 swarms, exhibited the lowest RMSE. Where, for all three models, the optimal number of lags was 2.

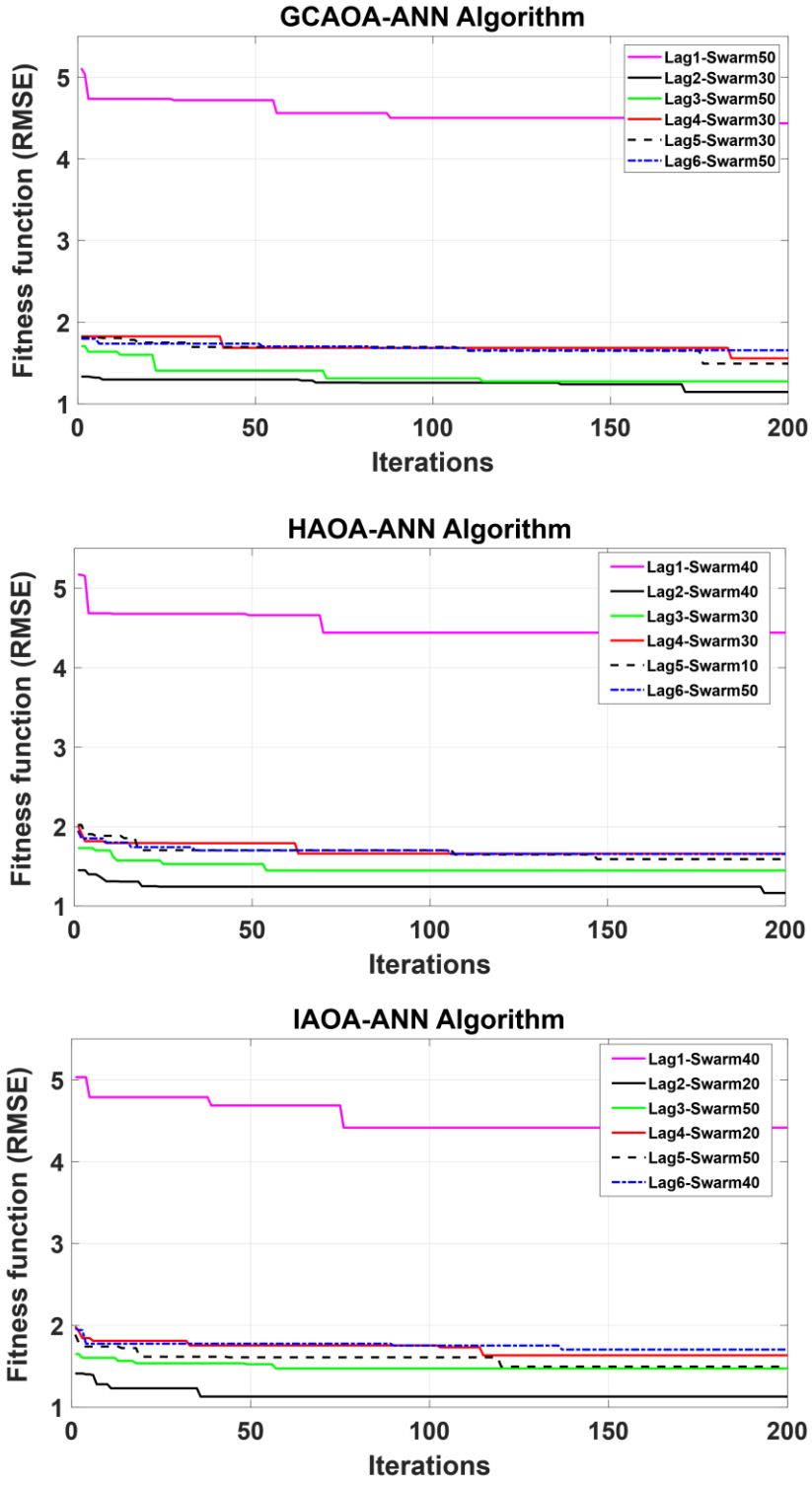

Figure 4. The optimal swarm for maximum temperature modelling using GCAOA, HAOA, and IAOA algorithms

The results of each MHA were used to fine-tune the ANN algorithm that simulates the maximum temperature. Table 2 displays the optimal population size for each situation, along with the ANN hyperparameters.

Table 2. ANN models' hyperparameters are offered by all MHAs

Model	Algorithm	Best swarm	N1	N2	LR
M2	IAOA-ANN	20	8	18	0.3374
	HAOA-ANN	40	3	3	0.2330
	GCAOA-ANN	30	16	19	2.375e-05

N1 and N2: Number of neurons in hidden layer one and two, and LR: ANN's learning rate.

Determining the number of neurons in the hidden layers is a critical step in designing ANNs. Excessively increasing the number of neurons can lead to information loss due to excessive complexity, while excessively decreasing it can limit the model's ability to represent data accurately. To overcome this problem, for example, the GCAOA algorithm was used to determine the optimal number of neurons, as shown in Table 2. The results showed that selecting the number of neurons in the two hidden layers (N1 and N2) directly impacts the model's accuracy. The GCAOA-ANN model, with 16 neurons in the first layer and 19 in the second, achieved the lowest RMSE, indicating a significant improvement in prediction accuracy. These results indicate that choosing the number of neurons must be done carefully, as any increase or decrease can lead to a decline in model performance.

3.2. Performance Assessment of Forecasting Techniques

The maximum temperature time series is divided into three portions. The first one (training) is used to build the ANN architecture (i.e., interlayer weights and biases), while the validation phase evaluates the architecture. The testing phase assesses the ANN's capacity to generalize to unseen data. To find the best ANN architecture for mimicking monthly maximum temperatures, all models were run multiple times after hyperparameter optimization, as shown in Table 2.

During the testing stage, several statistical metrics are used to assess and compare model performance. These metrics contain RMSE, NSC, max (error), MAE, MARE, NMSE, and R^2, as tabulated in Table 3. The table shows that all models perform well, but GCAOA-ANN outperforms the other two. The use of the GCAOA-ANN technique produces the lowest values of RMSE, max (error), MAE, and MRE. On the other hand, it produces the highest coefficients for NSC, NMSE, and R^2. For further comparison, two additional models, namely RF and XGBoost, were also utilized to confirm the performance of the hybrid models, and their results are shown in Table 3. In general, the hybrid models outperform RF and XGBoost, as they provide better predictions of the maximum temperatures across all statistical criteria.

Table 3. Evaluation of proposed models' performance throughout the testing data stage

Algorithm	RMSE °C	NSC	max(error) °C	MAE °C	MARE	NMSE	R^2
GCAOA-ANN	1.7354	0.969	3.9464	1.4527	0.0530	0.967	0.972
HAOA-ANN	2.0009	0.959	4.6646	1.5862	0.0583	0.954	0.963
IAOA-ANN	2.0653	0.956	4.1294	1.8184	0.0638	0.953	0.957
RF	2.8968	0.919	6.0282	2.2333	0.0764	0.077	0.919
XGBoost	3.8891	0.854	-6.8607	3.0522	0.1020	0.139	0.854

The suggested models underwent further testing to validate their capacity to predict the maximum temperature of Al-Hai City. As shown in Figure 5, there is a correlation between the simulated and observed temperature values. On the x-axis, the observed values are plotted versus the predicted values on the y-axis. The correlation coefficient (R) shows strong performance across all hybrid models, with R values greater than 0.97. The figure shows excellent agreement between the target (actual) and predicted data, with no anomalous points or obvious trends across all hybrid models, compared with the RF and XGBoost models, which show lower accuracy. The correlation coefficients are 0.986 for the GCAOA-ANN, 0.982 for the HAOA-ANN, and 0.978 for the IAOA-ANN model. On the other hand, the RF and XGBoost models yield lower correlation coefficients than the hybrid model (0.959 and 0.927, respectively).

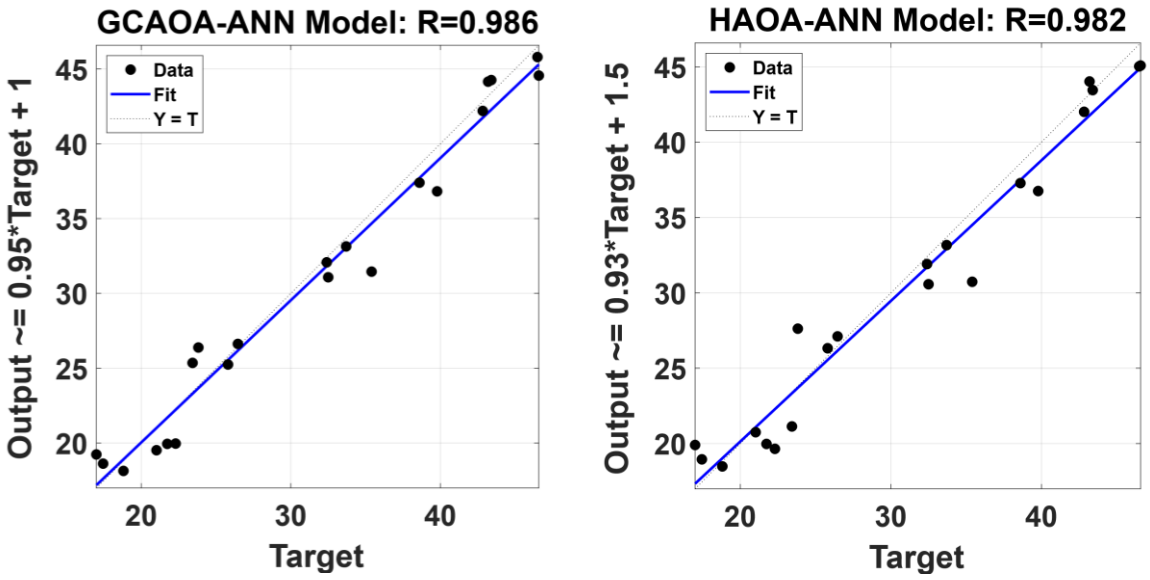

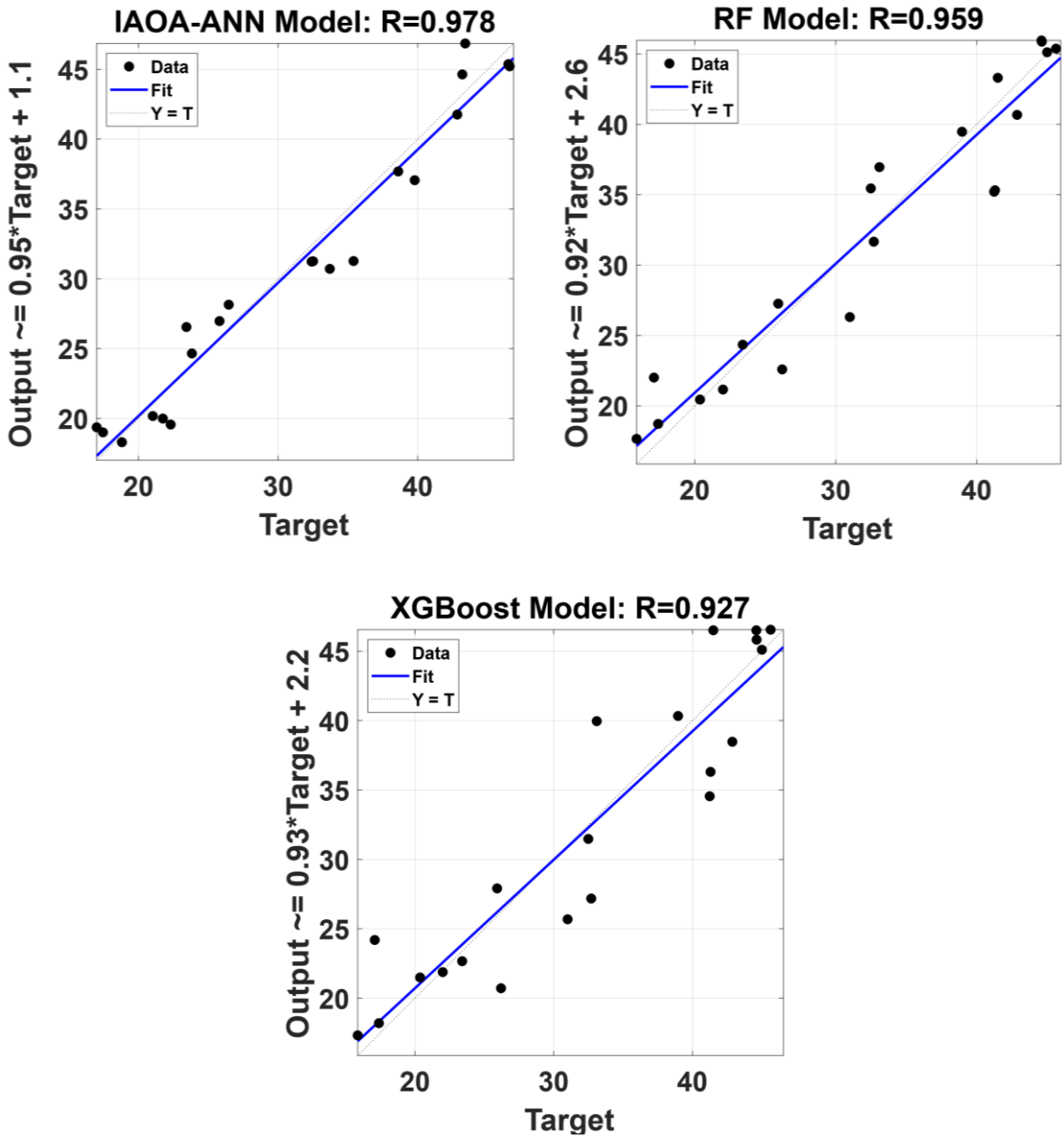

Figure 5. Graphical R test for all suggested hybrid techniques during the testing stage

This test verifies that the GCAOA-ANN model can accurately predict future maximum temperatures within the constraints outlined in the "Model validation" section. Compared with other hybrid models, the GCAOA-ANN model shows high consistency between observed and predicted data.

The results, shown in Table 3 and Figure 5, indicate that the hybrid model tends to perform better than the RF and XGBoost models in forecasting maximum temperatures during the testing phase. Accordingly, the remaining findings focus on confirming the superiority of the best hybrid ANN model. Figure 6-a illustrates the match between the actual temperature time series and the simulated time series from the three hybrid models during the testing phase. Although all the simulated series appear very close to the observed one (trend + periodicity), the GCAOA-ANN-predicted output is closest. This is also evident in Figure 6-b, which shows the error scatter plots. The error values for the GCAOA-ANN are mostly closer to zero than those from the other two models. This reflects the model's superiority. The error range can be estimated as (−2.564 to 3.946) °C, (−3.805 to 4.665) °C, and (−3.458 to 4.129) °C for the GCAOA-ANN, HAOA-ANN, and IAOA-ANN models, respectively. Also, no visible trend is exhibited in the scattered distribution.

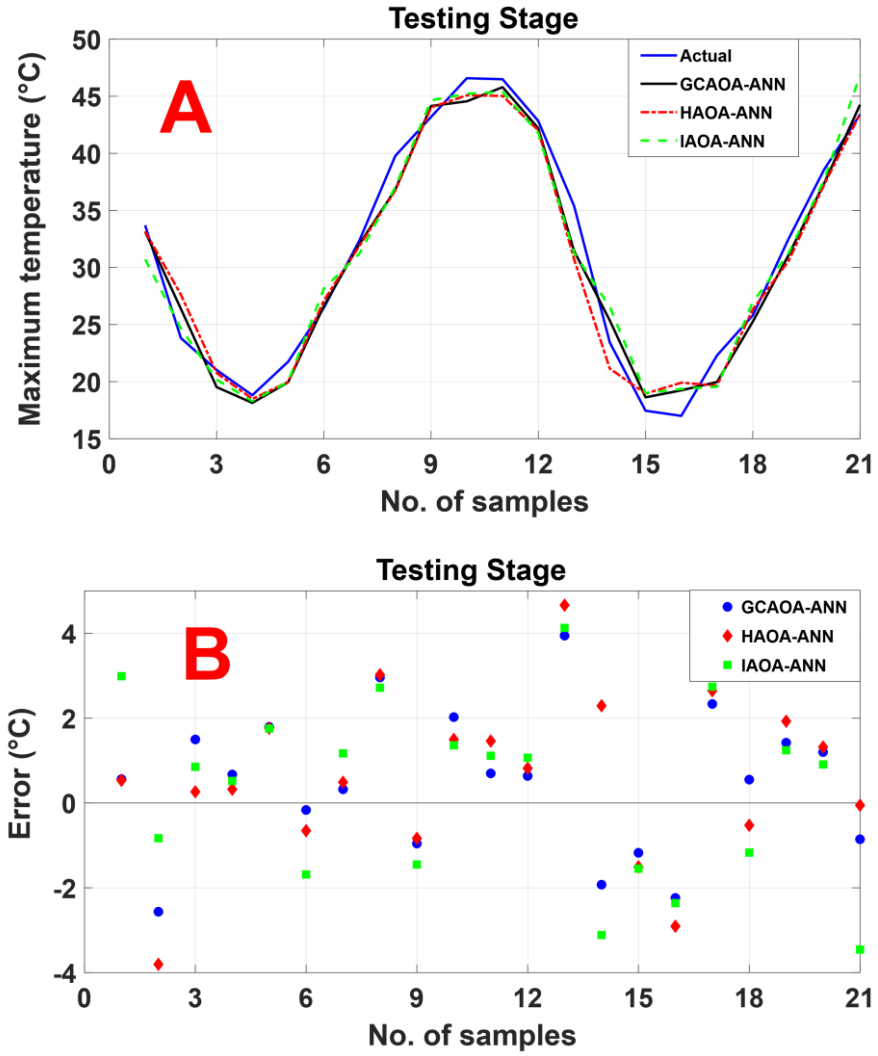

Figure 6. Shows (A) a comparison of actual and predicted maximum temperature time series and (B) residual scatterplots for the testing techniques of GCAOA-ANN, HAOA-ANN, and IAOA-ANN

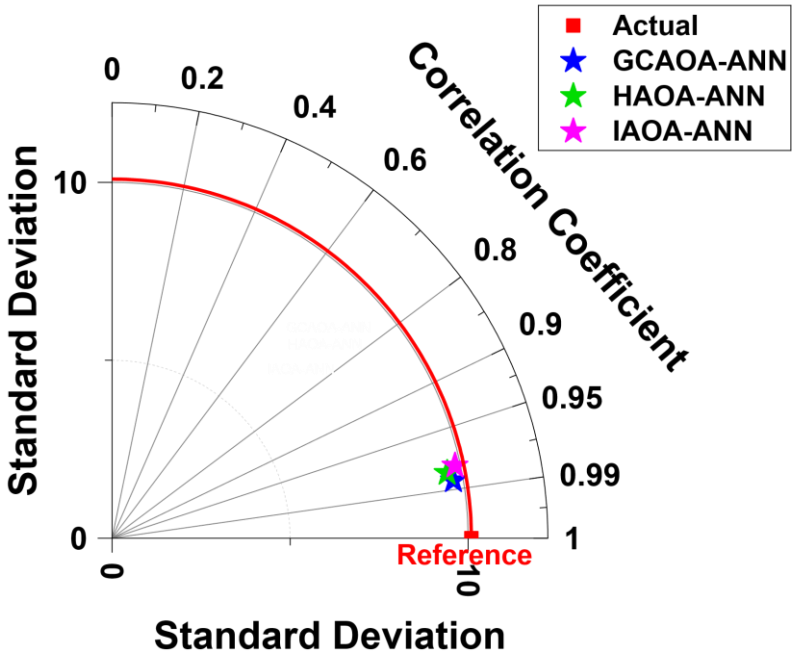

Figure 7. A Taylor diagram comparing the performances of the proposed hybrid techniques

The noise-robustness test results across different levels of artificial noise (SNR = 20, 25, and 30 dB) provide a comparative evaluation of the performance of the three hybrid models (GCAOA-ANN, HAOA-ANN, and IAOA-ANN). Figure 8 shows the behavior of the GCAOA-ANN model across ten independent trials at an SNR of 20 dB (i.e., simulated time series during the testing stage). The convergence and relative stability of the curves demonstrate the model's predictive performance consistency despite the random nature of the noise generation. To further illustrate the visual analysis, the corresponding statistical indicators are presented in Table 4. It should be noted that all values represent the average of 10 independent realizations at each SNR level, to minimize the effects of noise-generation randomness and enhance the reliability and statistical stability of the results.

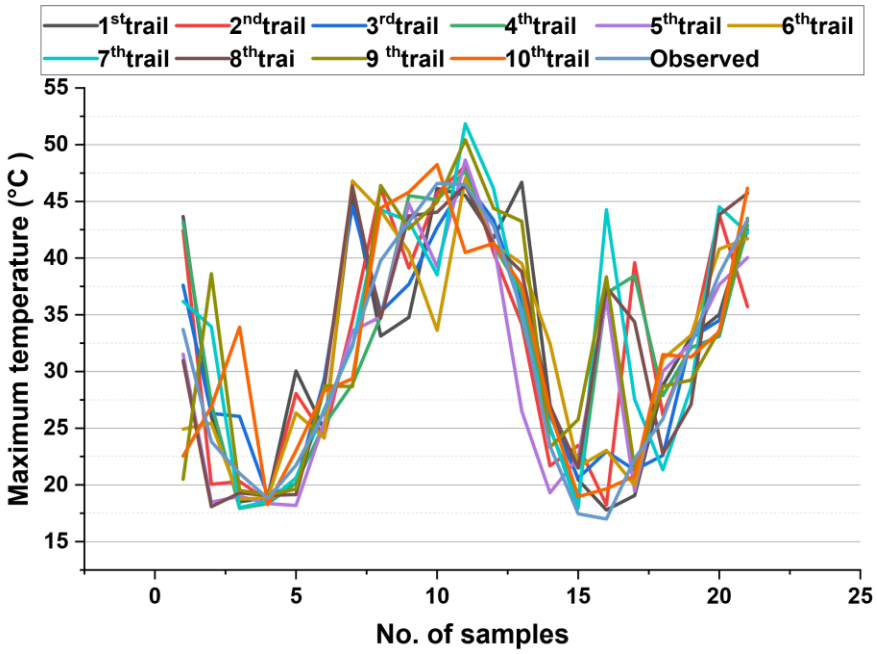

Figure 8. Results of ten independent trials of the GCAOA-ANN model at an SNR noise level of 20 dB and the observed testing time series

Table 4. Average performance criteria of forecast techniques considering three artificial noise (SNR = 20–30 dB)

GCAOA-ANN							
SNR (dB)	**RMSE °C**	**NSC**	**max(error) °C**	**MAE °C**	**MARE**	**NMSE**	**R^2**
20	5.9104	0.63	8.7085	4.059	0.154	0.626	0.684
25	3.551	0.864	6.1724	2.4364	0.0915	0.859	0.873
30	2.1407	0.951	3.6056	1.6499	0.0595	0.949	0.953
HAOA-ANN							
SNR (dB)	**RMSE °C**	**NSC**	**max(error) °C**	**MAE °C**	**MARE**	**NMSE**	**R^2**
20	7.0108	0.465	11.2207	4.9658	0.1892	0.44	0.566
25	3.6227	0.855	6.5033	2.4922	0.0928	0.839	0.866
30	2.5378	0.93	4.8509	1.9066	0.071	0.917	0.935
IAOA-ANN							
SNR (dB)	**RMSE °C**	**NSC**	**max(error) °C**	**MAE °C**	**MARE**	**NMSE**	**R^2**
20	7.3921	0.386	9.8088	4.6362	0.1767	0.492	0.584
25	5.4098	0.652	10.2115	3.4855	0.127	0.697	0.741
30	2.4975	0.929	3.8499	1.8799	0.0709	0.928	0.934

Error metrics (RMSE, MAE, and max(error)) decrease gradually as conformance coefficients (NSC, NMSE, and R^2) increase. However, a detailed comparison reveals a clear and consistent superiority of the GCAOA-ANN model across all tested noise levels. In the highest noise scenario (SNR = 20 dB), this model achieved the lowest errors and the highest conformance coefficients compared to the HAOA-ANN and IAOA-ANN models, demonstrating its superior ability to maintain predictive stability under severe input data disturbance.

As the noise level drops to a moderate level (SNR = 25 dB), this superiority becomes even more pronounced. The GCAOA-ANN model shows a marked improvement across all statistical indicators, with significant reductions in error and a rise in the coefficient of determination to levels indicating strong agreement between observed and predicted values. At SNR = 30 dB, representing a relatively low noise condition, the GCAOA-ANN model achieved the best overall performance among the three models, with the highest NSC and R^2 values and the lowest error metrics, indicating high predictive accuracy and excellent generalizability. Although the HAOA-ANN and IAOA-ANN models showed a gradual improvement in performance as noise decreased, their performance remained lower than that of the GCAOA-ANN model across all tested scenarios. This reflects the GCAOA-ANN model, which is robust to noise and continues to capture a large portion of the useful information in the time series.

4. Discussion

Developing reliable and accurate methods for determining maximum temperatures remains a hot topic of academic inquiry. To intervene effectively, decision-makers in Iraq require an accurate measure of maximum temperature, given the strong association between this variable and SDGs 2, 6, 11, and 13. Consequently, this research introduces a novel approach to monthly maximum temperature prediction using a multi-scenario methodology. One of the most important steps in designing ML approaches is determining the number of predictors, and our methodology has accounted for that. In this study, Table 1 presents six lag scenarios chosen as predictors, which are critical for precise maximum temperature forecasting. This agrees with Tran et al. [30] and Wang et al. [31], who recommended leveraging data usage in ANN applications by increasing the range of predictor variables, which significantly impacts ANN model robustness.

Hyperparameter optimization has also been shown to improve the predictive performance of ML models across various domains. Additionally, the superiority of hybrid-based MHAs compared with single-based ones, such as streamflow [68], water quality [22], and water level [23]. This paper has investigated three hybrid-based MHAs to choose the optimal ANN's hyperparameters, taking into account the shortcomings of hyperparameter optimization methods detailed in the "Introduction" section. These models are GCAOA-ANN, HAOA-ANN, and IAOA-ANN. Maximum temperature data were collected monthly and comprised 144 samples from Al-Hai City, Wasit Province, Iraq. These samples were divided into training, validation, and test sets.

During the ANN technique configuration, 1) the applied MHAs follow different techniques based on their performance during optimization. 2) Each configuration represents optimizing the model hyperparameters using MHA at a different number of swarms (each swarm repeated three times) and time series lagging order. Accordingly, the hybridization process generates multiple model scenarios, leading to a broad range of hyperparameter values. The best hybrid model configuration for each MHA is the one that minimizes RMSE across all configurations. Figure 4 reveals that the optimum set for lag and swarm numbers is lag2 with 30 swarms for GCAOA-ANN, lag2 with 40 swarms for HAOA-ANN, and lag2 with 20 swarms for the IAOA-ANN.

Based on the statistical and graphical tests used to assess the techniques during the testing phase (described in the "Results" section), all MHAs accurately reproduced maximum temperature data, according to Dawson et al. [65]. These findings support the literature's proposal [69, 70] that hybrid-based algorithms can solve real-world problems with greater accuracy, stability, and dependability while avoiding local minima. The superior performance probably results from 1) using a wide range of predictors' scenarios. 2) executing each algorithm's swarm three times. 3) applying three different MHAs that work with good strategies. For each of these factors, the outcome is a less uncertain and more robust range of predictions.

The hybrid models performed better than the RF and XGBoost models. However, the GCAOA-ANN outperformed the HAOA-ANN and IAOA-ANN techniques. The entire GCAOA-ANN model could predict the measured time series, and no significant distinctive points were observed in the predicted time series. This reflects the general good prediction. Also, the error analysis shows that the GCAOA-ANN had the lowest error values across the entire test sample compared to the other models. The key to the GCAOA-ANN model's superiority lies in its effective exploration and exploitation strategies, which leverage IGOL and DE/best/2/bin to escape local optima and expand undiscovered areas in the feature space. Moreover, the lower and upper bounds are updated using the best knowledge from the optimal solutions, thereby significantly reducing the number of iterations required to reach a global solution. Finally, the developed four arithmetic operations, along with their control parameters, assist the decision-maker in finding the optimal solution during the optimization process. As a result, the hybrid GCAOA algorithm plays an essential role in selecting optimal hyperparameters for the ANN mode, achieving very high accuracy and stability and boosting convergence rate.

The noise robustness test results based on SNR (20–30 dB) confirm that the GCAOA-ANN model exhibits higher predictive stability compared to other hybrid models, particularly under conditions of high noise and input data uncertainty. This is crucial in climate modeling, where historical data are often affected by noise and measurement errors. This superiority can be attributed to the GCAOA algorithm's ability to achieve a more effective balance between exploration and exploitation during neural network parameter optimization, thus reducing localized fallout and improving generalizability. In contrast, the HAOA-ANN and IAOA-ANN models showed greater sensitivity to

increasing noise levels, as reflected in their relative performance decline under high-noise scenarios. Furthermore, repeating the test 10 times at each SNR level provided a more reliable assessment of model robustness, as the average values reflect the overall model behavior rather than results from a single noise realization. Accordingly, the results highlight the importance of assessing model robustness under artificially generated disturbance conditions rather than relying on nominal accuracy measures, and support the adoption of the GCAOA-ANN model as a more reliable predictive framework for handling turbulent climate data.

The findings in this study are subject to at least two limitations, but those could be valuable in future investigations. First, the study uses only 12 years of monthly maximum temperature data, which may limit generalizability. Second, the model relies solely on lagged temperature values (univariate approach). In terms of future work, it would be interesting to focus on longer datasets or higher-frequency (daily/hourly) data. Additionally, assess the impact of using additional meteorological variables (e.g., humidity, wind speed) on improving predictive performance for maximum temperatures. Notwithstanding the relatively limited sample, this work offers valuable insights into predicting maximum temperatures under noise-robustness constraints.

The efficacy of various hybrid MHAs that incorporate other ML methods, such as support vector regression and random forests, could be the subject of future research. These results may contribute to a better understanding and forecasting of how maximum temperatures vary, which helps policy-makers support the SDGs. It is useful in agricultural planning, water management, disaster protection, and improving climate adaptation strategies.

5. Proposed Policies for Decision-Makers

In light of the findings of this study, a set of proposed policies can be presented to support decision-makers in addressing the challenges of climate change, particularly concerning extreme temperatures and their environmental and economic impacts:

- Adopting AI-based hybrid models, such as the GCAOA-ANN model, to forecast extreme temperatures, given their high accuracy in reducing error and improving forecast performance.
- Establishing comprehensive, long-term climate databases to support predictive models based on multiple time-lag scenarios improves the models' ability to capture climate patterns accurately.
- Developing AI-based early warning systems to address extreme climate events, such as heat waves and droughts, thus contributing to reducing environmental and human damage.
- Enhancing integration between predictive models and vital sectors, such as agriculture, water resources management, and energy, to facilitate informed strategic decisions based on accurate data.
- Linking predictive model outputs to the Sustainable Development Goals (SDGs), particularly those related to climate (SDG13), water (SDG6), food (SDG2), and sustainable cities (SDG11), to ensure that environmental policies are aligned with the international development agenda.

6. Conclusion

Interest in modeling needs has been on the rise due to the growing need to accurately depict maximum temperatures in fields such as medicine, agriculture, energy, and climate research. The present study compared the forecasting performance of three combined ML systems for monthly maximum temperatures at the Al-Hai City station in Iraq. The three models combined ANN with hybrid-based metaheuristic algorithms, including GCAOA-ANN, HAOA-ANN, and IAOA-ANN. Various combinations of input scenarios were tested with different lag periods (from lag1 to lag6). Hybridization produces varying hyperparameter values, which, in turn, yield distinct ANN model scenarios, because the MHAs used for optimization follow diverse strategies. Several possible explanations account for why, on the whole, all the prediction methods worked well. This advantage may exist, for example, because different permutations of input scenarios produce more precise forecasts.

Another probable explanation is that the optimal solution was found by running each algorithm's swarm three times, yielding a wider range of forecasts and reduced uncertainty. Seven statistical tests (i.e., RMSE, MAE, MARE, max(error), NSC, NMSE, and R^2) and four graphical tests (i.e., R, residual scatter plot, time series comparison, and Taylor diagram) were applied to assess the prediction models. In general, the lag2 (M2) provides an accurate model across all hybrid models, and the optimal swarm sizes are 20, 30, and 40 for the IAOA-ANN, GCAOA-ANN, and HAOA-ANN, respectively. According to the test-stage results, the predicted and actual values show good correspondence for all proposed models, with R^2, NSC, and NMSE all high and within (0.972-0.957), (0.969-0.956), and (0.967-0.953), respectively. The RF and XGBoost techniques were applied, and their results were compared with those of hybrid models. The findings (Table 3 and Figure 5) reveal that the hybrid model performed better than other models. However, GCAOA-ANN outperformed HAOA-ANN and IAOA-ANN models across different tests, achieving the highest correspondence between actual and forecasted data and the lowest error, as tabulated in Table 3 and Figures 5, 6, and 7.

Furthermore, the results of this study were enhanced by an additional noise-robustness test that added artificial noise to the test data at signal-to-noise ratios (SNR) of 20, 25, and 30 dB to simulate different levels of uncertainty in the input data. The results of this test showed that all models were affected by increasing noise levels. However, the GCAOA-ANN model maintained the best performance across all tested SNR levels, with the lowest error metrics and the highest fit coefficients. This behavior confirms that the superiority demonstrated by the GCAOA-ANN model is not limited to ideal data conditions but extends to cases of severe data disturbance, reflecting higher predictive stability and generalizability and enhancing the model's reliability for practical applications in climate forecasting. The research helps develop precise decision priorities. It can streamline valuation and forecasting techniques for weather records, which are crucial to various meteorological, environmental, and climatological research projects. It would be beneficial to conduct additional research on studies that utilize ML models combined with hybrid metaheuristic algorithms to predict better how Earth's environment will evolve in the future, as climate change is a hot topic in these areas right now. It should be noted that additional studies are needed to account for a wide range of geological conditions, model types, and input factors. Sustainable water resources and agricultural systems can be enhanced using additional meteorological variables.

7. Declarations

7.1. Author Contributions

Conceptualization, S.L.Z. and H.A.; methodology, A.W.A. and H.M.R.; software, H.M.R.; validation, M.A. and H.A.H.; formal analysis, A.W.A. and S.L.Z.; investigation, H.A. and H.M.R.; resources, S.L.Z.; data curation, H.A.; writing—original draft preparation, A.W.A., S.L.Z., and H.A.; writing—review and editing, M.A. and H.A.H.; visualization, S.L.Z. and H.A. All authors have read and agreed to the published version of the manuscript.

7.2. Data Availability Statement

The data presented in this study are available on request from the corresponding author.

7.3. Funding

The authors received no financial support for the research, authorship, and/or publication of this article.

7.4. Conflicts of Interest

The authors declare no conflict of interest.

8. References

[1] Bhih, M., Elassad, Z. E. A., Siti, H., Meslouhi, O. E. L., Abouelmehdi, K., & Boustani, A. El. (2026). Temporal pattern-aware temperature forecasting using CatBoost: A hybrid machine learning approach. Results in Engineering, 30. doi:10.1016/j.rineng.2026.110212.

[2] Jalal, H. K., Hassan, W. H., & Nile, B. K. (2026). Spatiotemporal dynamics and future projections of aridity in a semi-arid region based on multi-model CMIP6 scenarios. Theoretical and Applied Climatology, 157(1), 20. doi:10.1007/s00704-025-05977-z.

[3] Hadi, S. H., Alwan, H. H., & Al-Mohammed, F. M. (2024). Analysis of Climate Change Scenarios Using the LARS-WG 8 Model Based on Precipitation and Temperature Trends. Civil Engineering Journal (Iran), 10(12), 4019–4042. doi:10.28991/CEJ-2024-010-12-014.

[4] Shah, V., Patel, N., Shah, D., Swain, D., Mohanty, M., Acharya, B., Gerogiannis, V. C., & Kanavos, A. (2024). Forecasting Maximum Temperature Trends with SARIMAX: A Case Study from Ahmedabad, India. Sustainability (Switzerland), 16(16). doi:10.3390/su16167183.

[5] United Nations (2025) Sustainable Development Goals: 17 Goals to Transform Our World. United Nations, New York, United States. Available online: https://www.un.org/en/exhibits/page/sdgs-17-goals-transform-world (accessed on May 2026).

[6] Choi, B., Bergés, M., Bou-Zeid, E., & Pozzi, M. (2021). Short-term probabilistic forecasting of meso-scale near-surface urban temperature fields. Environmental Modelling & Software, 145. doi:10.1016/j.envsoft.2021.105189.

[7] Hou, J., Wang, Y., Zhou, J., & Tian, Q. (2022). Prediction of hourly air temperature based on CNN–LSTM. Geomatics, Natural Hazards and Risk, 13(1), 1962–1986. doi:10.1080/19475705.2022.2102942.

[8] Zhou, L., Chen, H., Xu, L., Cai, R. H., & Chen, D. (2024). Deep learning-based postprocessing for hourly temperature forecasting. Meteorological Applications, 31(2), 2194. doi:10.1002/met.2194.

[9] Gomes, O. S., Binelo, M. O., Binelo, M. D. F. B., Oliveira, J. P. C., Galvani, E., & Alves, R. R. (2025). An Artificial Neural Network for Short Time Air Temperature Prediction. IEEE Access, 13, 77593–77598. doi:10.1109/ACCESS.2025.3565731.

[10] Topcu, A. E., AlQallaf, M. K. I., Alzoubi, Y. I., & Elbasi, E. (2026). Machine learning models for predicting daily temperature extremes. European Journal of Sustainable Development Research, 10(3), em0396. doi:10.29333/ejosdr/18318.

[11] Sevgin, F. (2025). Machine Learning-Based Temperature Forecasting for Sustainable Climate Change Adaptation and Mitigation. Sustainability (Switzerland), 17(5). doi:10.3390/su17051812.

[12] Elbeltagi, A., Vishwakarma, D. K., Katipoğlu, O. M., Sushanth, K., Heddam, S., Singh, B. P., Shukla, A., Gautam, V. K., Pande, C. B., Hussain, S., Ghosh, S., Dehghanisanij, H., & Salem, A. (2025). Air temperature estimation and modeling using data driven techniques based on best subset regression model in Egypt. Scientific Reports, 15(1), 20200. doi:10.1038/s41598-025-06277-2.

[13] Arslan, R. U., Aksoy, B., & Yapıcı, İ. Ş. (2026). Temperature trend prediction with explainable artificial intelligence and PCA based machine learning: a case study of Zonguldak, Turkey. Scientific Reports, 16(1), 4910. doi:10.1038/s41598-026-35173-6.

[14] Tikhamarine, Y., Malik, A., Pandey, K., Sammen, S. S., Souag-Gamane, D., Heddam, S., & Kisi, O. (2020). Monthly evapotranspiration estimation using optimal climatic parameters: efficacy of hybrid support vector regression integrated with whale optimization algorithm. Environmental Monitoring and Assessment, 192(11), 696. doi:10.1007/s10661-020-08659-7.

[15] Ahmadi, F., Mehdizadeh, S., & Mohammadi, B. (2021). Development of Bio-Inspired- and Wavelet-Based Hybrid Models for Reconnaissance Drought Index Modeling. Water Resources Management, 35(12), 4127–4147. doi:10.1007/s11269-021-02934-z.

[16] Elbeltagi, A., Kushwaha, N. L., Rajput, J., Vishwakarma, D. K., Kulimushi, L. C., Kumar, M., Zhang, J., Pande, C. B., Choudhari, P., Meshram, S. G., Pandey, K., Sihag, P., Kumar, N., & Abd-Elaty, I. (2022). Modelling daily reference evapotranspiration based on stacking hybridization of ANN with meta-heuristic algorithms under diverse agro-climatic conditions. Stochastic Environmental Research and Risk Assessment, 36(10), 3311–3334. doi:10.1007/s00477-022-02196-0.

[17] Merchaoui, M., Sakly, A., & Mimouni, M. F. (2018). Particle swarm optimisation with adaptive mutation strategy for photovoltaic solar cell/module parameter extraction. Energy Conversion and Management, 175, 151–163. doi:10.1016/j.enconman.2018.08.081.

[18] Chen, H., Jiao, S., Wang, M., Heidari, A. A., & Zhao, X. (2020). Parameters identification of photovoltaic cells and modules using diversification-enriched Harris hawks optimization with chaotic drifts. Journal of Cleaner Production, 244, 244. doi:10.1016/j.jclepro.2019.118778.

[19] Ridha, H. M. (2020). Parameters extraction of single and double diodes photovoltaic models using Marine Predators Algorithm and Lambert W function. Solar Energy, 209, 674–693. doi:10.1016/j.solener.2020.09.047.

[20] Hanoon, M. S., Ahmed, A. N., Zaini, N., Razzaq, A., Kumar, P., Sherif, M., Sefelnasr, A., & El-Shafie, A. (2021). Developing machine learning algorithms for meteorological temperature and humidity forecasting at Terengganu state in Malaysia. Scientific Reports, 11(1), 18935. doi:10.1038/s41598-021-96872-w.

[21] Khairan, H. E., Zubaidi, S. L., Muhsen, Y. R., & Al-Ansari, N. (2023). Parameter Optimisation-Based Hybrid Reference Evapotranspiration Prediction Models: A Systematic Review of Current Implementations and Future Research Directions. Atmosphere, 14(1). doi:10.3390/atmos14010077.

[22] Khudhair, Z. S., Zubaidi, S. L., Ortega-Martorell, S., Al-Ansari, N., Ethaib, S., & Hashim, K. (2022). A Review of Hybrid Soft Computing and Data Pre-Processing Techniques to Forecast Freshwater Quality's Parameters: Current Trends and Future Directions. Environments, 9(7), 85. doi:10.3390/environments9070085.

[23] Mohammed, S. J., Zubaidi, S. L., Ortega-Martorell, S., Al-Ansari, N., Ethaib, S., & Hashim, K. (2022). Application of hybrid machine learning models and data pre-processing to predict water level of watersheds: Recent trends and future perspective. Cogent Engineering, 9(1), 2143051. doi:10.1080/23311916.2022.2143051.

[24] Ridha, H. M., Hizam, H., Mirjalili, S., Othman, M. L., Ya'acob, M. E., Ahmadipour, M., & Ismaeel, N. Q. (2022). On the problem formulation for parameter extraction of the photovoltaic model: Novel integration of hybrid evolutionary algorithm and Levenberg Marquardt based on adaptive damping parameter formula. Energy Conversion and Management, 256, 115403. doi:10.1016/j.enconman.2022.115403.

[25] Ridha, H. M., Hizam, H., Mirjalili, S., Othman, M. L., & Ya'acob, M. E. (2022). Zero root-mean-square error for single- and double-diode photovoltaic models parameter determination. Neural Computing and Applications, 34(14), 11603–11624. doi:10.1007/s00521-022-07047-1.

[26] Ridha, H. M., Hizam, H., Mirjalili, S., Othman, M. L., Ya'acob, M. E., & Abualigah, L. (2022). A Novel Theoretical and Practical Methodology for Extracting the Parameters of the Single and Double Diode Photovoltaic Models. IEEE Access, 10, 11110–11137. doi:10.1109/ACCESS.2022.3142779.

[27] Astsatryan, H., Grigoryan, H., Poghosyan, A., Abrahamyan, R., Asmaryan, S., Muradyan, V., Tepanosyan, G., Guigoz, Y., & Giuliani, G. (2021). Air temperature forecasting using artificial neural network for Ararat valley. Earth Science Informatics, 14(2), 711–722. doi:10.1007/s12145-021-00583-9.

[28] Alomar, M. K., Khaleel, F., Aljumaily, M. M., Masood, A., Razali, S. F. M., AlSaadi, M. A., Al-Ansari, N., & Hameed, M. M. (2022). Data-driven models for atmospheric air temperature forecasting at a continental climate region. Plos One, 17(11), e0277079. doi:10.1371/journal.pone.0277079.

[29] Johnstone, C., & Sulungu, E. D. (2021). Application of neural network in prediction of temperature: a review. Neural Computing and Applications, 33(18), 11487–11498. doi:10.1007/s00521-020-05582-3.

[30] Tran, T. T. K., Bateni, S. M., Ki, S. J., & Vosoughifar, H. (2021). A review of neural networks for air temperature forecasting. Water (Switzerland), 13(9), 1294. doi:10.3390/w13091294.

[31] Wang, H., Yang, J., Chen, G., Ren, C., & Zhang, J. (2023). Machine learning applications on air temperature prediction in the urban canopy layer: A critical review of 2011–2022. Urban Climate, 49. doi:10.1016/j.uclim.2023.101499.

[32] Zhang, H., Liu, Y., Zhang, C., & Li, N. (2025). Machine Learning Methods for Weather Forecasting: A Survey. Atmosphere, 16(1), 82. doi:10.3390/atmos16010082.

[33] Al-Ansari, N. (2020). Topography and Climate of Iraq. Journal of Earth Sciences and Geotechnical Engineering, 11(2), 1–13. doi:10.47260/jesge/1121.

[34] Abdullah, M., Al-Ansari, N., & Laue, J. (2020). Water harvesting in Iraq: Status and opportunities. Journal of Earth Sciences and Geotechnical Engineering, 10(1), 199-217.

[35] Jasim, I. A., Hasan, H. M., Farhan, S. L., & Bahat, K. H. (2021). Evaluating the urban structure of Al-Kut city according to sustainability. IOP Conference Series: Earth and Environmental Science, 779(1), 12021. doi:10.1088/1755-1315/779/1/012021.

[36] Khairan, H. E., Zubaidi, S. L., Al-Mukhtar, M., Dulaimi, A., Al-Bugharbee, H., Al-Faraj, F. A., & Ridha, H. M. (2023). Assessing the Potential of Hybrid-Based Metaheuristic Algorithms Integrated with ANNs for Accurate Reference Evapotranspiration Forecasting. Sustainability (Switzerland), 15(19), 14320. doi:10.3390/su151914320.

[37] Hassan, W. H., Nile, B. K., Kadhim, Z. K., Mahdi, K., Riksen, M., & Thiab, R. F. (2023). Trends, forecasting and adaptation strategies of climate change in the middle and west regions of Iraq. SN Applied Sciences, 5(12), 312. doi:10.1007/s42452-023-05544-z.

[38] Muhaisen, N. Kh., Khayyun, T. Sh., Al Mukhtar, M., & Hassan, W. H. (2024). Forecasting changes in precipitation and temperatures of a regional watershed in Northern Iraq using LARS-WG model. Open Engineering, 14(1), 20220567. doi:10.1515/eng-2022-0567.

[39] Jalal, H. K., Hassan, W. H., & Nile, B. K. (2025). Projected the Impacts of Climate Change on the Unconfined Aquifer Region, Western Iraq, Using LARS-WG and CMIP6 Scenarios. Water Conservation Science and Engineering, 10(2), 84. doi:10.1007/s41101-025-00410-y.

[40] Khalaf, R. M., Hussein, H. H., Hassan, W. H., Mohammed, Z. M., & Nile, B. K. (2022). Projections of precipitation and temperature in Southern Iraq using a LARS-WG Stochastic weather generator. Physics and Chemistry of the Earth, Parts A/B/C, 128, 103224. doi:10.1016/j.pce.2022.103224.

[41] Dheyaa, M. A., Al-Mukhtar, M. M., & Shemal, K. (2024). Analyzing the Future Climate Change Impacts on Meteorological Parameters Using the LARS-WG Model. Civil Engineering Journal, 10(11), 3754–3778. doi:10.28991/CEJ-2024-010-11-019.

[42] Mohammed, Z. M., & Hassan, W. H. (2022). Climate change and the projection of future temperature and precipitation in southern Iraq using a LARS-WG model. Modeling Earth Systems and Environment, 8(3), 4205–4218. doi:10.1007/s40808-022-01358-x.

[43] Habib, M. K., & Cherri, A. K. (1998). Parallel quaternary signed-digit arithmetic operations: Addition, subtraction, multiplication and division. Optics & Laser Technology, 30(8), 515–525. doi:10.1016/S0030-3992(99)00004-3.

[44] Xu, Y. P., Tan, J. W., Zhu, D. J., Ouyang, P., & Taheri, B. (2021). Model identification of the Proton Exchange Membrane Fuel Cells by Extreme Learning Machine and a developed version of Arithmetic Optimization Algorithm. Energy Reports, 7, 2332–2342. doi:10.1016/j.egyr.2021.04.042.

[45] Del Ser, J., Osaba, E., Molina, D., Yang, X. S., Salcedo-Sanz, S., Camacho, D., Das, S., Suganthan, P. N., Coello Coello, C. A., & Herrera, F. (2019). Bio-inspired computation: Where we stand and what's next. Swarm and Evolutionary Computation, 48, 220–250. doi:10.1016/j.swevo.2019.04.008.

[46] Mahdavi, S., Rahnamayan, S., & Deb, K. (2018). Opposition based learning: A literature review. Swarm and Evolutionary Computation, 39, 1–23. doi:10.1016/j.swevo.2017.09.010.

[47] Abd Elaziz, M., & Oliva, D. (2018). Parameter estimation of solar cells diode models by an improved opposition-based whale optimization algorithm. Energy Conversion and Management, 171, 1843–1859. doi:10.1016/j.enconman.2018.05.062.

[48] Xu, S., & Wang, Y. (2017). Parameter estimation of photovoltaic modules using a hybrid flower pollination algorithm. Energy Conversion and Management, 144, 53–68. doi:10.1016/j.enconman.2017.04.042.

[49] Karafotias, G., Hoogendoorn, M., & Eiben, A. E. (2015). Parameter Control in Evolutionary Algorithms: Trends and Challenges. IEEE Transactions on Evolutionary Computation, 19(2), 167–187. doi:10.1109/TEVC.2014.2308294.

[50] Bilal, Pant, M., Zaheer, H., Garcia-Hernandez, L., & Abraham, A. (2020). Differential Evolution: A review of more than two decades of research. Engineering Applications of Artificial Intelligence, 90, 103479. doi:10.1016/j.engappai.2020.103479.

[51] Al-Dabbagh, R. D., Neri, F., Idris, N., & Baba, M. S. (2018). Algorithmic design issues in adaptive differential evolution schemes: Review and taxonomy. Swarm and Evolutionary Computation, 43, 284–311. doi:10.1016/j.swevo.2018.03.008.

[52] Yang, X., Gong, W., & Wang, L. (2019). Comparative study on parameter extraction of photovoltaic models via differential evolution. Energy Conversion and Management, 201, 112113. doi:10.1016/j.enconman.2019.112113.

[53] Humphries, N. E., Queiroz, N., Dyer, J. R. M., Pade, N. G., Musyl, M. K., Schaefer, K. M., Fuller, D. W., Brunnschweiler, J. M., Doyle, T. K., Houghton, J. D. R., Hays, G. C., Jones, C. S., Noble, L. R., Wearmouth, V. J., Southall, E. J., & Sims, D. W. (2010). Environmental context explains Lévy and Brownian movement patterns of marine predators. Nature, 465(7301), 1066–1069. doi:10.1038/nature09116.

[54] Mantegna, R. N. (1994). Fast, accurate algorithm for numerical simulation of Lévy stable stochastic processes. Physical Review E, 49(5), 4677–4683. doi:10.1103/PhysRevE.49.4677.

[55] Oliva, D., Abd El Aziz, M., & Ella Hassanien, A. (2017). Parameter estimation of photovoltaic cells using an improved chaotic whale optimization algorithm. Applied Energy, 200, 141–154. doi:10.1016/j.apenergy.2017.05.029.

[56] Kamaruddin, M., Manullang, M. C. T., & Yee, J.-J. (2025). Integrating Gradient Boosting and Parametric Architecture for Optimizing Energy Use Intensity in Net-Zero Energy Buildings. Civil Engineering Journal, 11(3), 910–931. doi:10.28991/CEJ-2025-011-03-06.

[57] Guo, Q., He, Z., & Wang, Z. (2024). Monthly climate prediction using deep convolutional neural network and long short-term memory. Scientific Reports, 14(1), 17748. doi:10.1038/s41598-024-68906-6.

[58] Bayatvarkeshi, M., Mohammadi, K., Kisi, O., & Fasihi, R. (2020). A new wavelet conjunction approach for estimation of relative humidity: wavelet principal component analysis combined with ANN. Neural Computing and Applications, 32(9), 4989–5000. doi:10.1007/s00521-018-3916-0.

[59] Zare Abyaneh, H., Bayat Varkeshi, M., Golmohammadi, G., & Mohammadi, K. (2016). Soil temperature estimation using an artificial neural network and co-active neuro-fuzzy inference system in two different climates. Arabian Journal of Geosciences, 9(5), 377. doi:10.1007/s12517-016-2388-8.

[60] Cifuentes, J., Marulanda, G., Bello, A., & Reneses, J. (2020). Air temperature forecasting using machine learning techniques: A review. Energies, 13(6). doi:10.3390/en13164215.

[61] Ghorbani, M. A., Deo, R. C., Karimi, V., Yaseen, Z. M., & Terzi, O. (2018). Implementation of a hybrid MLP-FFA model for water level prediction of Lake Egirdir, Turkey. Stochastic Environmental Research and Risk Assessment, 32(6), 1683–1697. doi:10.1007/s00477-017-1474-0.

[62] Zubaidi, S. L., Kumar, P., Al-Bugharbee, H., Ahmed, A. N., Ridha, H. M., Mo, K. H., & El-Shafie, A. (2023). Developing a hybrid model for accurate short-term water demand prediction under extreme weather conditions: a case study in Melbourne, Australia. Applied Water Science, 13(9), 184. doi:10.1007/s13201-023-01995-2.

[63] Seo, Y., Kwon, S., & Choi, Y. (2018). Short-Term Water Demand Forecasting Model Combining Variational Mode Decomposition and Extreme Learning Machine. Hydrology, 5(4), 54. doi:10.3390/hydrology5040054.

[64] Li, M. W., Xu, R. Z., Yang, Z. Y., Hong, W. C., An, X. G., & Yeh, Y. H. (2024). Optimization approach of berth-quay crane-truck allocation by the tide, environment and uncertainty factors based on chaos quantum adaptive seagull optimization algorithm. Applied Soft Computing, 152, 111197. doi:10.1016/j.asoc.2023.111197.

[65] Dawson, C. W., Abrahart, R. J., & See, L. M. (2007). HydroTest: A web-based toolbox of evaluation metrics for the standardised assessment of hydrological forecasts. Environmental Modelling & Software, 22(7), 1034–1052. doi:10.1016/j.envsoft.2006.06.008.

[66] Pan, M., Zhou, H., Cao, J., Liu, Y., Hao, J., Li, S., & Chen, C. H. (2020). Water Level Prediction Model Based on GRU and CNN. IEEE Access, 8, 60090–60100. doi:10.1109/ACCESS.2020.2982433.

[67] Ren, T., Liu, X., Niu, J., Lei, X., & Zhang, Z. (2020). Real-time water level prediction of cascaded channels based on multilayer perception and recurrent neural network. Journal of Hydrology, 585, 124783. doi:10.1016/j.jhydrol.2020.124783.

[68] Kareem, B. A., Zubaidi, S. L., Al-Ansari, N., & Muhsen, Y. R. (2024). Review of Recent Trends in the Hybridisation of Preprocessing-Based and Parameter Optimisation-Based Hybrid Models to Forecast Univariate Streamflow. CMES - Computer Modeling in Engineering & Sciences, 138(1), 1–41. doi:10.32604/cmes.2023.027954.

[69] Zeinolabedini Rezaabad, M., Ghazanfari, S., & Salajegheh, M. (2020). ANFIS Modeling with ICA, BBO, TLBO, and IWO Optimization Algorithms and Sensitivity Analysis for Predicting Daily Reference Evapotranspiration. Journal of Hydrologic Engineering, 25(8), 04020038. doi:10.1061/(asce)he.1943-5584.0001963.

[70] El-kenawy, E. S. M., Zerouali, B., Bailek, N., Bouchouich, K., Hassan, M. A., Almorox, J., Kuriqi, A., Eid, M., & Ibrahim, A. (2022). Improved weighted ensemble learning for predicting the daily reference evapotranspiration under the semi-arid climate conditions. Environmental Science and Pollution Research, 29(54), 81279–81299. doi:10.1007/s11356-022-21410-8.